Full Paper

Medium Temperature Shift Reaction Over Copper-Ceria Catalyst in Fixed-Bed and Microchannel Reactors

A. Irankhah [1], Y. Davoodbeygi [2]*

[1] *Hydrogen and Fuel Cell Research Laboratory, Department of Chemical Engineering, Faculty of Engineering, University of Kashan, Kashan, Iran*
[2] *Department of Chemical Engineering, University of Hormozgan, Bandar Abbas, Iran*

ARTICLE INFO

ABSTRACT

One of the effective catalysts for the hydrogen purification and production via medium temperature shift reaction, is Cu-Ce solid solution. $Cu_{0.1}Ce_{0.9}O_{1.9}$ was produced using the co-precipitation method and then was utilized as support for the $5Cu/Ce_{0.9}Cu_{0.1}O_{1.9}$ catalyst which was synthesized employing the wet impregnation method. The X-ray diffraction (XRD) analysis showed that the crystalline sizes of $Ce_{0.9}Cu_{0.1}O_{1.9}$ and $5Cu/Cu_{0.1}Ce_{0.9}O_{1.9}$ were 9.22 and 18.33 nm respectively. The Catalysts were evaluated in medium temperature shift reaction at 300-390 °C and at the gas hourly space velocities (GHSV) of 12000 and 30000 h^{-1}, in a fixed bed reactor. Due to the higher concentration of Cu and the positive synergic effects of both the active metal and support, the $5Cu/Cu_{0.1}Ce_{0.9}O_{1.9}$ catalyst showed a better performance. It was also concluded that, because of the short residence time at high levels of GHSV, increasing GHSV would lead to a decrease in the CO conversion. Then $5Cu/Cu_{0.1}Ce_{0.9}O_{1.9}$ was evaluated in a microchennel reactor in 2 GHSVs of 12000 and 30000 h^{-1} and results were compared with thoes of the fixed-bed reactor. It can be concluded that the microchannel reactor is better in higher GHSVs (shorter residence time of the gas flow). A microchannel reactor provides a high surface-to-volume ratio and gases pass over the thin layer of catalysts on the coated plates. Hence, due to the better access to the catalytic bed, the reactants react even in a short time, which improves the performance of the microchannel compared to that of the fixed bed reactor.

1. Introduction
In current limitations of the conventional fuels additional to environmental concerns, increases the demand of their replacement with

---

renewable sources of energy [1]. Fuel cells are promising devices to convert the stored chemical energy directly to the electrical energy [2]. Proton exchange membrane fuel cells (PEMFCs) use hydrogen to produce electricity [3]. Hydrogen is obtainable from natural gas [4], methanol, ethanol and etc. [5], via processes such as steam reforming [4], partial oxidation [6] and autothermal reforming [7]. Nonetheless, by the mentioned processes there are some amounts of carbon monoxide in the formed hydrogen stream, which can cause the poisoning of the anode catalyst in PEMFC [6]. The water gas shift (WGS) reaction is applied to purify and also produce hydrogen ($CO+H_2O \rightarrow H_2+CO_2$) [8]. The WGS reaction commonly involves two stages of the low temperature shift (LTS, at the temperatures between of 150 to 250 °C and catalyzed by Cu-Zn-Al) [9], and the high temperature shift (HTS, at the temperatures between of 350 to 450 °C and catalyzed by Fe-Cr) [10]. These two stages can be altered by a medium temperature shift (MTS) reaction executed at between 280 to 360 °C [11]. The most common catalysts for the MTS reaction are catalysts such as Pt, Au, Cu and Ni, supported on porous oxides like ZrO_2, CeO_2 and TiO_2 [12]. As reported in literatures, Cu-Ce catalysts showed good performances in the water gas shift (WGS) reaction [13]. In fact Cu-Ce mixed oxide as a consequence of its high activity, which is the result of the high capacity of the oxygen mobility of CeO_2 and the powerful interaction of metal and support between Cu species and the oxygen vacancies of ceria lattice [14, 15].

One of the important parameters in the design of reactors is to minimize the mass and heat transfer resistances as well as the sufficient residence time to perform the reaction. [16, 17]. In fixed bed reactors, the catalysts are often loaded randomly, which may lead to a non-uniform flow pattern, non-uniform access of the reactant to the catalyst active sites, and thus a reduction in the performance of the reactor. Creating hot spots is also a possible problem in using fixed bed reactors. In order to overcome the mentioned problems, the use of microreactors, in which a layer of catalyst is placed on the plates of the microreactors, is suggested [18]. The electrophoretic deposition (EPD) method is used for a wide range of coating processes, in which the charged particles are disperesed in a liquid phase, then in the applied electric field, the particles are dipositted on the electrode with the opposite charge [19]. There are few reports on applying the EPD coating method in microreactors for catalytic processes. Yang. et al. [20] preapered pouros layers of alumina by couting an aluminium powder layer on stainless steel using the EPD technique. Nodeyalkova et al. [21] investigated the EPD coating of the cobalte based catalyst in ethanol steam reforming. Mohammadnezami et al. [22] applied the EPD method to coat the Ni-based catalyst for the methane steam reforming process. They investigated the voltage and coating time as important variables of the EPD process and reported 120 V and 1.5 min as optimum values for the voltage and coating time respectively. They also found that under the mentioned optimum condition, the performance of the micro-reformer was better than that of the packed-bed reactor. Recently, the EPD method was applied for coating the nickel based catalyst on ceria support on stainless steel using a microreactor in order to perform the water gas shift reaction [23], and in another study [24] the effect of solvents in the EPD method was also investigated.

This work presents an evaluation of the

copper-ceria mixed oxide in the MTS process. At the start the $Ce_{0.9}Cu_{0.1}O_{1.9}$ catalyst is produced by the co-precipitation method, then it is applied as support for synthesizing $5Cu/Ce_{0.9}Cu_{0.1}O_{1.9}$ by the wet impregnation method. Furthermore, the effect of GHSV on the catalytic performance of the mentioned catalysts in the MTS reaction is studied. Finally Cu-Ce mixide oxide is coated on stailess steel plates by the EPD method, and the catalytic performance in a microchannel reactor is compared with the fixed bed reactor.

2. Experimental
2.1. Catalysts preparation and characteristics
In order to synthesis the $Ce_{0.9}Cu_{0.1}O_{1.9}$ catalyst via the co-precipitation method, chosen quantities of $Ce(NO_3)_3.6H_2O$ (99 % LOBA Chemie), and $Cu(NO_3)_2.3H_2O$ (LOBA Chemie), were dissolved in distillated water. The produced mixture and precipitation agent (the sodium carbonate solution) were simultaneously added to a beaker containing surfactant (0.5 wt % poly ethylene glycol (PEG) in distillated water). The pH was kept at approximately 7 during the precipitation process. The produced precipitate was digested for 8 hours at room temperature, after that it was dried at 80 °C for 18 hours and finally calcined at 450 °C with the heating rate of 3 °C/min for 4 h. the $5Cu/Ce_{0.9}Cu_{0.1}O_{1.9}$ catalyst was prepared by the wet impregnation method. An appropriate amount of $Cu(NO_3)_2.3H_2O$ was added to the solution containing the co-precipitated $Ce_{0.9}Cu_{0.1}O_{1.9}$, as support, and distilled water. The mixture was stirred for 4 hours at room temperature. The drying and calcination conditions are the same as the above mentioned for the $Ce_{0.9}Cu_{0.1}O_{1.9}$ prepared by the co-precipitation method. To achieve the XRD recorded patterns

of the samples, an X-ray diffractometer (P Analytical X'Pert-Pro) with a Cu Kα monochromatized radiation source and a Ni filter, in the 2θ range of 20-80° was deployed. The Brunauer-Emmett-Teller (BET) analysis was used to obtain the catalyst surface area using an automated gas adsorption analyzer (Tristar3020; Micrometrics) with the N_2 adsorption at the temperature of −196 °C. Furthermore, a hydrogen temperature programmed reduction (H_2-TPR) test was performed using the Micromeritics Chemisorb 2750 apparatus equipped with a thermal conductivity detector (TCD). 0.02 g of the sample was pretreated under 40 mL/min of the Argon flow. Then 10 % H_2 in Ar was introduced at a flow rate of 30 mL/min with a heating rate of 10 °C/min to increase the temperature from room temperature to 1000 °C.

2.2. Feed and reaction conditions
Figure 1 shows the process flow diagram (PFD) of the MTS reaction. The feed contains a mixture of 14.3 mol % carbon monoxide and 71.4 mol % hydrogen balanced with Argon. It should be mentioned that the total dry feed flow rate was 70 ml/min and the molar ratio of steam to carbon monoxide was kept at 3.0. To study the effect of GHSV on the catalytic performance, the experiments were performed in 2 GHSVs of 12000 and 30000 h^{-1}. Before performing each test, the catalysts were reduced for 1 hour under the pure hydrogen flow (30 cm^3/min) at 400 °C.

All of the flows, were analyzed by a gas chromatograph apparatus (GC), Shimadzu-8A (Hysep Q column), with a TCD.

The CO conversion was calculated as follow:

$$CO \ conversion = \{[F_{CO \ in} - F_{CO \ out}]/F_{CO \ in}\} \times 100 \quad (1)$$

where $F_{CO \ out}$ and $F_{CO \ in}$ are respectively the

flow rate of CO in the outlet and inlet streams (mol/s). It should be mentioned that no
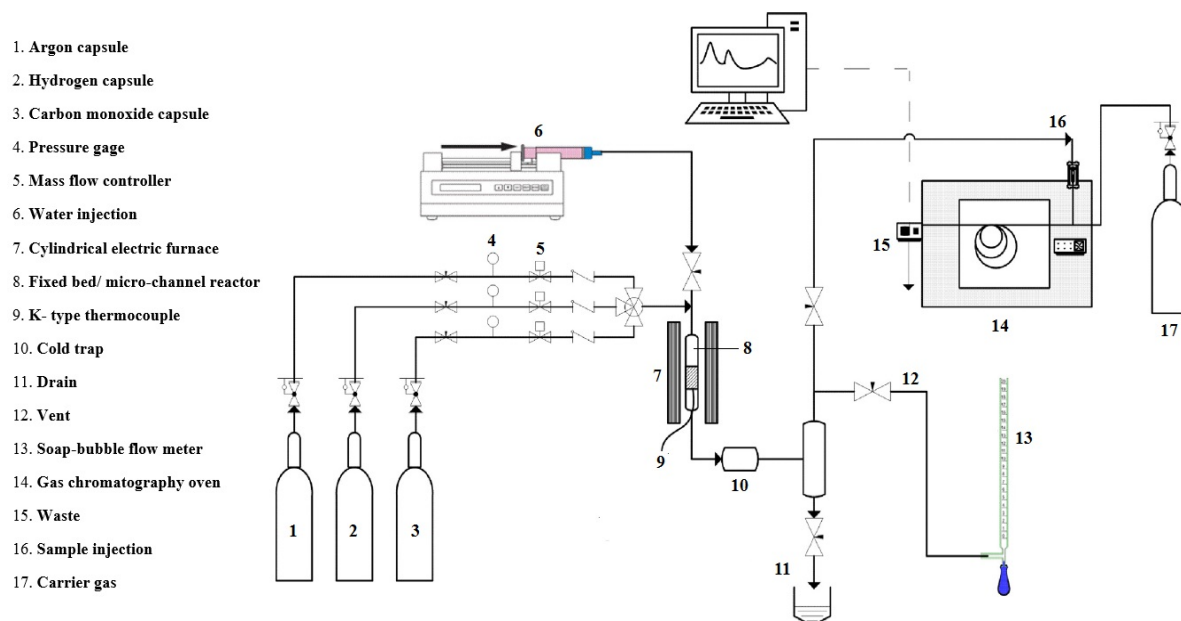
methane production was detected in tests.

1. Argon capsule
2. Hydrogen capsule
3. Carbon monoxide capsule
4. Pressure gage
5. Mass flow controller
6. Water injection
7. Cylindrical electric furnace
8. Fixed bed/ micro-channel reactor
9. K- type thermocouple
10. Cold trap
11. Drain
12. Vent
13. Soap-bubble flow meter
14. Gas chromatography oven
15. Waste
16. Sample injection
17. Carrier gas

Figure 1. Process flow diagram for the rector tests of the MTS reaction.

2.3. Reactors: Fixed bed and microchannel

In this study, two types of the fixed bed quartz reactor and microchannel stainless steel reactor have been used to evaluate the catalytic performance of Cu-Ce in the MTS reaction. In fixed bed tests, 0.5 g of the catalyst with the mesh size of 40-60 (250-460 micron) was planted in a quartz reactor with internal diameter of 8 mm. in order to perform tests related to the catalytic evaluation in the microchannel, the coated plates were fixed between two stainless steel microstructured walls with a splitting-jointing pattern, which was designed and manufactured by Mahmoudizadeh et al. [19].

2.4. EPD coating of microchannel plates

The preparation of the suspension and the procedure of EPD: In order to prepare the suspension, first a certain amount of the desired catalyst is milled at 180 rpm for 15 min, in a planetary ball mill with a 1:20 powder-to-ball weight ratio, and then it is

added to a solution containing isopropanol (Loba Chemie) and polyethylenimine (PEI, Sigma Aldrich) as the dispersion medium and stabilizer respectively. The resulted mixture was stirred on a magnetic plate stirrer with a speed of 400 rpm for 15 min. Afterwards, in order to make the suspension more uniform and prevent the agglomeration of particles, it was sonicated (1200M, Soltec) for 15 minutes. Stainless steel plates (SUS304) have been used as electrodes for the EPD process. First, 2.2×3.2 cm^2 metal plates with a thickness of 1 mm were cut, washed, polished and sonicated with acetone. In order to EPD coat, the electrodes are immersed vertically in the beaker containing the suspension and by applying an electric field, the powder settles on one of the electrodes. The deposition process starts by pressing the power switch and setting up the circuit. The optimum conditions for the EPD process were reported by Bazdar et al. [23] as follows: Coating was carried out in the suspension with 3 wt % catalyst powder in a

140 V electric field for 3 min, and distance between two electrodes was pf 1.5 cm. After the deposition process, in order to create more stable layer and remove impurities, all plates were placed in a furnace at 400 °C for 2 h.

3. Results and discussion

The XRD patterns of $Ce_{0.9}Cu_{0.1}O_{1.9}$ and $5Cu/Ce_{0.9}Cu_{0.1}O_{1.9}$ catalysts are shown in Figure 2. It is obvious that the peaks in $Ce_{0.9}Cu_{0.1}O_{1.9}$ sample are shorter and wider than thoes in the impregnated one, which indicates a smaller crystalline size. The average crystalline size of catalysts, which was determined by the Scherrer's equation, was 9.23 and 18.32 nm for $Ce_{0.9}Cu_{0.1}O_{1.9}$ and $5Cu/Ce_{0.9}Cu_{0.1}O_{1.9}$ samples, respectively.
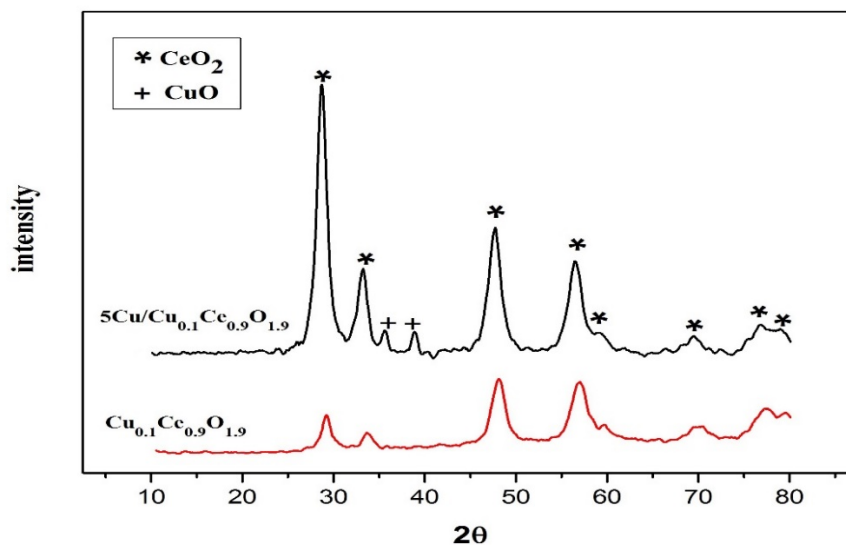
Figure 2. XRD patterns of $Ce_{0.9}Cu_{0.1}O_2$ and $5Cu/Ce_{0.9}Cu_{0.1}O_2$ catalysts.

The SEM images of $Ce_{0.9}Cu_{0.1}O_{1.9}$ and $5Cu/Ce_{0.9}Cu_{0.1}O_{1.9}$ catalysts are shown in Figure 3. Evidently, the impregnating of Cu on the Ce-Cu support results in larger particles, which is due to the copper agglomeration on the support. However the presence of Cu active sites is higher in the impregnated sample, which can significantly affect the catalytic performance.
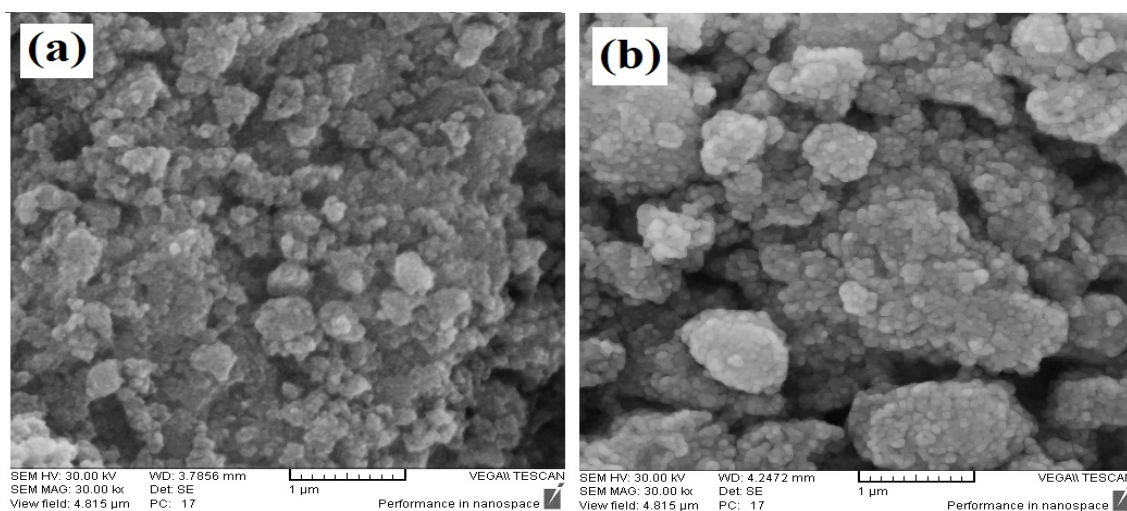

Figure 3. SEM images of a) $Ce_{0.9}Cu_{0.1}O_{1.9}$, and b) $5Cu/Ce_{0.9}Cu_{0.1}O_{1.9}$ catalysts.

Figure 4 shows the reactor test results for $Ce_{0.9}Cu_{0.1}O_{1.9}$ and $5Cu/Ce_{0.9}Cu_{0.1}O_{1.9}$ catalysts in two different GHSVs in the MTS reaction using the fixed bed reactor. As it is obvious in this figure, the impregnation of 5 wt % Cu on the precipitated $Ce_{0.9}Cu_{0.1}O_{1.9}$ leads to an increase in the CO conversion at the whole range of temperatures and also at both examined GHSVs. As a matter of fact, although the impregnated sample has larger crystalline size (about two times larger than $Ce_{0.9}Cu_{0.1}O_{1.9}$), because of more active Cu sites and more availability of them for the reactants, this sample showed a better performance. It is also concluded from the experimental results that for both samples, the CO conversion decreases by increasing the GHSV. In the high GHSV, the residence time is short and the reactants don't have enough time for the reaction.
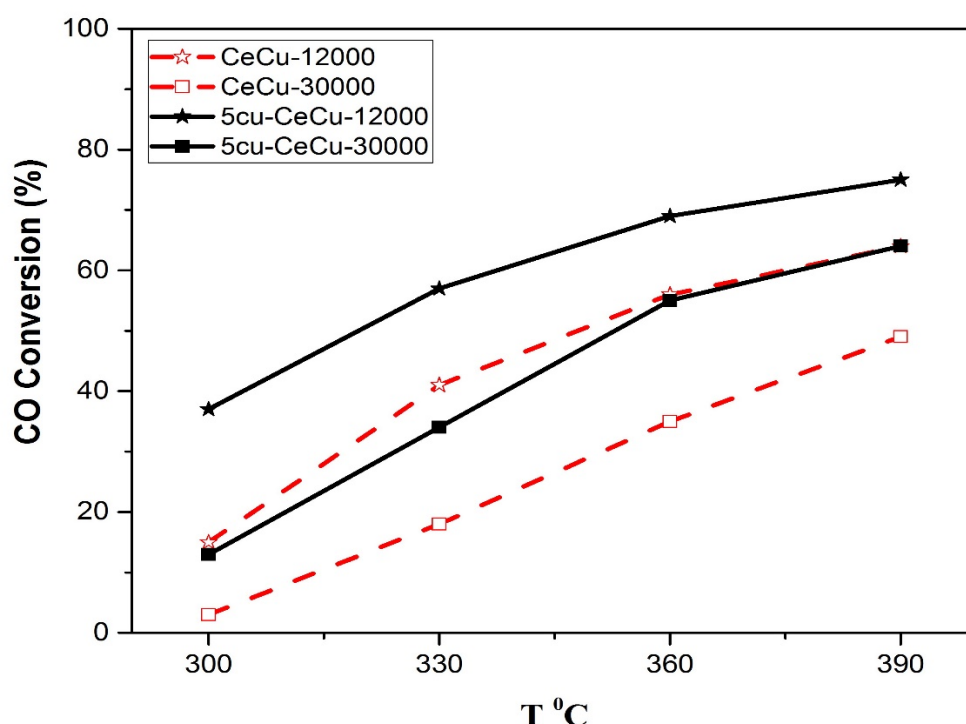

Figure 4. CO conversion versus temperature for $Ce_{0.9}Cu_{0.1}O_{1.9}$ and $5Cu/Ce_{0.9}Cu_{0.1}O_{1.9}$ catalysts at different GHSVs, the atmospheric pressure and S/C = 3 in the fixed-bed reactor.

According to the mentioned results, $5Cu/Ce_{0.9}Cu_{0.1}O_{1.9}$ was selected for being evaluated in the microchannel reactor. Figure 5 shows further characteristics of this sample. The nitrogen adsorption/desorption isotherm of the $5Cu/Ce_{0.9}Cu_{0.1}O_{1.9}$ catalyst is shown in Figure 5-a, which is in the IV type classification (mesoporous materials) with an H3 hysteresis loop. The pore size distribution is also shown in Figure 5-a. It should be mentioned that this sample has the BET surface area = 54.05 m^2/g, pore volume = 0.1554 cm^3/g, and mean pore size = 12.32 nm. The TPR diagram of $5Cu/Ce_{0.9}Cu_{0.1}O_{1.9}$, shown in Figure 5-b, provides 4 peaks. Peak "d" at about 850 °C refferes to Ceria species. At the temperature of 100 to 300 °C, 3 peaks, which correspond to CuO and Cu-Ce mixed oxides, can be seen. Peak "a" is related to the superficial CuO, Peak "b" is associated with the strong interaction of CuO and ceria oxygen vacancies, and Peak "c" corresponds to the type of CuO which is entering the ceria lattice without any bonding [25].
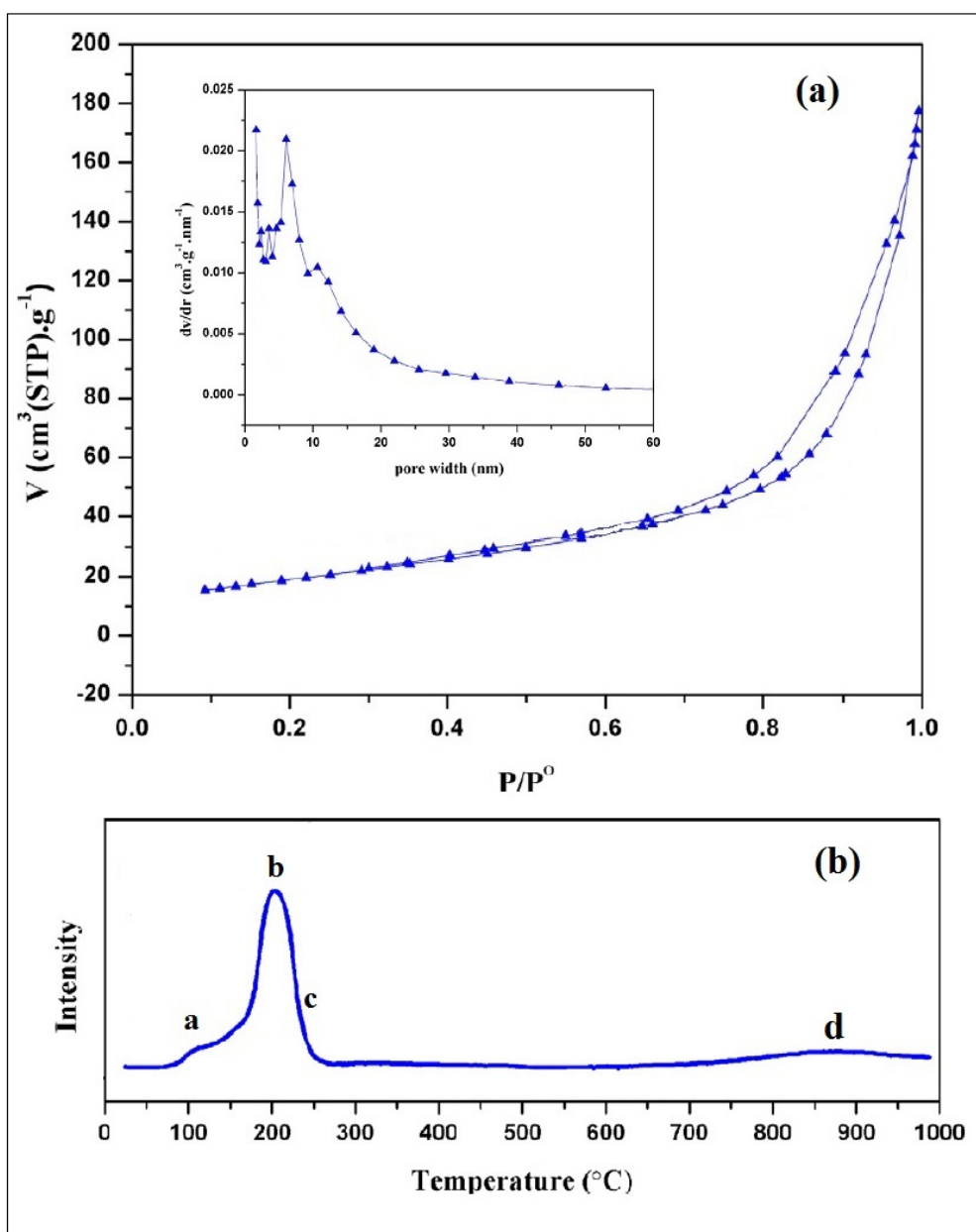
Figure 5. $5Cu/Ce_{0.9}Cu_{0.1}O_{1.9}$ further characteristics analysis a) the BET analysis: the N_2 adsorption-desorption versus P/P0, and the pore size distribution, b) the TPR diagram.

Figure 6 shows the performance of the $5Cu/Ce_{0.9}Cu_{0.1}O_{1.9}$ catalyst in the MTS reaction in the fixed bed and microrechannel reactors. The experiments were performed on the two GHSVs of 12000 and 30000 h^{-1}. As it is obvious in this figure, at the GHSV of 12000 h^{-1}, the catalytic performance in the fixed bed reactor has been better, but at the GHSV of 30000 h^{-1}, the microchannel has performed better. It is obvious that as the GHSV increases, the residence time of the gas

flow descreases and the gas velocity increases. In fact, the better performance of the microchannel reactor in high GHSVs is due to the high reatio of surface to volume in the microchannel reactor and the gas passing over the thin layer of the catalyst on the coated plates, which causes the reactants react even in a short time due to the better access to the catalytic bed, which improves the performance of the microchannel compared to that of the fixed bed reactor.
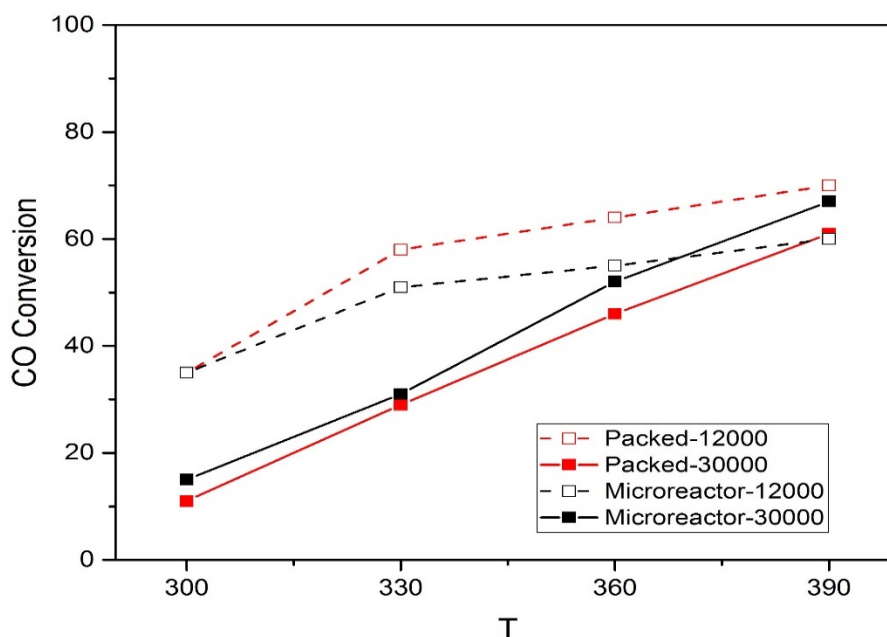
Figure 6. CO conversion versus temperature for the $5Cu/Ce_{0.9}Cu_{0.1}O_{1.9}$ catalyst at different GHSVs, the atmospheric pressure and S/C = 3, in the fixed-bed and microchannel reactors.

4. Conclusions

For the hydrogen purification and production, medium temperature shift reaction was applied over Cu-Ce mixed oxide, at the temperature of 300 to 390 °C and the atmospheric pressure, in the fixed bed and microchannel reactors. $Ce_{0.9}Cu_{0.1}O_{1.9}$ was prepared by the differential co-precipitation method and used as a support for the impregnation of 5 wt % of Cu on it. The crystalline size of $Ce_{0.9}Cu_{0.1}O_{1.9}$ and $5Cu/Ce_{0.9}Cu_{0.1}O_{1.9}$, calculated by the Scherrer equation, were 9.22 and 18.33 nm respectively. The results of the fixed-bed reactor tests showed a better performance for $5Cu/Ce_{0.9}Cu_{0.1}O_{1.9}$ sample, which is due to 2 points; one is the higher concentration and better dispersion of Cu as the active metal, and the other one is the positive synergic effects of the active metal and support on the catalytic performance. The effect of GHSV was also investigated in 2 levels of 12000 and 30000 h^{-1}. Results showed that the CO conversion decreased by increasing GHSV which was related to the short residence time at the high levels of GHSV. Then $5Cu/Cu_{0.1}Ce_{0.9}O_{1.9}$ was tested in a microchannel reactor in the 2 GHSVs of 12000 and 30000 h^{-1}. Results were compared with those of the fixed-bed reactor. It can be concluded that in high GHSVs, due to the short residence time and the high gas velocity, the microchannel reactor showed a better performance. On account of the high ratio of surface to volume in the microchannel reactor and the gas passing over the thin layer of the catalyst on the coated plates, the reactants react even in a short time. The reason of it is related to the better access to the catalytic bed, which improves the performance of the microchannel reactor compared to that of the fixed bed reactor.

Nomenclature

BET   Brunauer-Emmet-Teller.
EPD   Elctrophoretic Deposition.
GC   Gas Chromatography.
GHSV   Gas Hourly Space Velocity.
HTS   High Temperature Shift.
MTS   Medium Temperature Shift.
LTS   Low Temperature Shift.
PEG   Plolyethylene Glycole.
PEMFC Protin Exchange Membrane Fuel Cell.
PEI   PolyethyLenimine.
PFD   Process Flow Diagram.
TCD   Thermal Conductivity Detector.
TPR   Temperature Programmed Reduction.
WGS   Water Gas Shift.
XRD   X-Ray Diffraction.

References

[1] Chen, W. -H. and Chen, C. -Y., "Water gas shift reaction for hydrogen production and carbon dioxide capture: A review", *Applied Energy*, **258**, 114078 (2020).

[2] Das, V., Padmanaban, S., Venkitusamy, K., Selvamuthkumaran, R., Blaabjerg, F. and Siano, P., "Recent advancces and challenges of fuel cell based power system architectures and control- A review", *Renewable and Sustainable Energy Reviews*, **73**, 10 (2017).

[3] Chavan, S. L. and Talange, D. B., "Modeling and performance evaluation of PEM fuel cell by controlling its input parameters", *Energy*, **138**, 437 (2017).

[4] Anzelmo, B., Wilcox, J. and Liguori, S., "Hydrogen production via natural gas steam reforming in a Pd-Au membrane reactor: Comparison between methane and natural gas steam reforming reactions", *Journal of Membrane Science*, **568**, 113 (2018).

[5] Holladay, J. D., Hu, J., King, D. L. and Wang, Y., "An overview of hydrogen production production", *Catalysis Today*, **139,** 244 (2009).

[6] Singha, R. K., Shukla, A., Yadav, A., Konathala, L. N. S. S. and Bal, R., "Effect of metal-support interaction on activiry and stability of Ni-CeO2 catalyst for partial oxidation of methane", *Applied Catalysid B: Environmental*, **202**, 473 (2017).

[7] Carapellucci, R. and Giordano, L., "Steam dry and autothermal methane reforming for hydrogen production: A thermodynamic equilibrium analysis", *Journal of Power Sources*, **469**, 228391 (2020).

[8] Pal, D. B., Chand, R., Upadhyay, S. N. and Mishra, P. K., "Performance of water gas shift reaction catalysts: A review", *Renewable and sustainable Energy Reviews*, **93**, 549 (2018).

[9] Shim, J. -O., Na, H. -S., Ahn, S. -Y., Jeon, K. -W., Jeon, B. -H. and Roh, H. -S., "An important parameter for synthesis of Al_2O_3 supported Cu-Zn catalysts in low temperature water-gas shift reaction under particular reaction condition", *International Journal of Hydrogen Energy*, **44**, 14853 (2019).

[10] Martos, C., Dufour, J. and Ruiz, A., "Synthesis of Fe_3O_4-based catalysts for the high-temperature water gas shift reaction", *International Journal of Hydrogen Energy*, **34**, 4475 (2009).

[11] Alijani, A. and Iankhah, A., "Medium temperature shift catalysts for hydrogen purification in a single-stage reactor", *Chemical Engineering Technology*, **36**, 209 (2013).

[12] Irankhah, A., Heidari, F. and Davoodbeygi, Y., "Synthesis, characterization, and evaluation of nickel catalysts on nanocrystalline CeO_2 promoted by K and Mn for medium-temperature shift reaction and hydrogen purification", *Research on Chemical Intermediates*, **43**, 7119 (2017).

[13] Davoodbeygi, Y. and Irankhah, A., "Catalytic characteristics of $Ce_xCu_{1-x}O_{1.9}$ catalysts formed by solid state method for MTS and OMTS reactions", *International Journal of Hydrogen Energy*, **44**, 16443 (2019).

[14] Davoodbeygi, Y. and Irankhah, A., "Nanostructured Ce-Cu mixed oxide synthesized by solid state reaction for medium temperature shift reaction: Optimization using response surface method", *International Journal of Hydrogen Energy*, **43**, 22218 (2018).

[15] Li, L., Song, L., Chen, C., Zhang, Y., Zhan, Y., Lin, X., Zheng, Q., Wang, H., Ma, H., Ding, L. and Zhu, W., "Modified precipitation processes and optimized copper content of $CuO-CeO_2$ catalysts for water-gas shift reaction", *International Journal of Hydrogen Energy*, **39**, 19570 (2014).

[16] Rahimi, M., Azimi, N., Parsamoghadam, M. A., Rahimi, A. and Mashay, M. M., "Mixing performance of T, Y, and oriented Y-micromixers with spatially arranged outlet channel: Evaluation with Villermaux/Dushman test reaction", *Microsyst Technol.*, **23**, 3117 (2017).

[17] Hosseini Khalvandi, F., Rahimi, M., Jafari, O. and Azimi, N., "Liquid-liquid two-phase mass transfer in T-type micromixers with different junctions and cylindrical pits", *Chemical Engineering and Processing*, **107**, 58 (2016).

[18] Mellie, V., "Review on methods to deposit catalysts on structured surfaces", *Applied Catalysis A: General*, **315**, 1 (2006).

[19] Mahmoudizadeh, M., Irankhah, A., Irankhah, R. and Jafari, M., "Development of a replaceable microreractor coated with a CuZnFe nanocatalyst for methanol steam reforming", *Chemical Engineering Technology*, **39**, 322 (2016).

[20] Yang, K. S., Jiang, Z. and Chung, J. S., "Electrophoretically Al-coated wire mesh and its application for catalytic oxidation of 1,2-dichlorobenzene", *Surface Coating Technology,* **168**, 103 (2003).

[21] Neyalkova, R., Casanovas, A., Liorca, J. and Montane, D., "Electrophoretic deposition of Co-Me/ZnO(Me[Mn, Fe]) ethanol steam reforming catalysts on stainless steel plates", *International Journal of Hydrogen Energy*, **34**, 25934 (2009).

[22] Mohammadnezami, H. and Irankhah, A., "Electrophoretic coating for steam methane micro-reformer: Optimum voltage and time, channel design, and substrate type", *International Journal of Energy Research*, **45**, 15980 (2021).

[23] Bazdar, M. and Irankhah, A., "Performance study on microchannel coated catalytic plate reactor using electrophoresis technique for medium temperature shift (MTS) reaction", *Energy & Fuels*, **31**, 7624 (2017).

[24] Bazdar, M. and Irankhah, A, "Water gas shift reaction in a microchannel Ni-based catalytic coated reactor: Effect of solvent", *Chem. Eng. Technology*, **43**, 2428 (2020).

[25] Cheshmeh-Roshan, A., Irankhah, A., Mahmoudizadeh, M. and Arandiyan, H., "Single-stage water gas shift reaction over structural modified Cu-Ce catalysts at medium temperatures: Synthesis and catalyst performance", *Chemical Engineering Research and Design*, **132**, 843 (2018).